Exploring Lubrication Regimes at the Nanoscale: Nanotribological Characterization of Silica and Polymer Brushes in Viscous Solvents

ARTICLE *in* LANGMUIR · JULY 2013

Impact Factor: 4.46 · DOI: 10.1021/la402148b · Source: PubMed

4 AUTHORS, INCLUDING:

Nicholas D Spencer
ETH Zurich
403 PUBLICATIONS **11,621** CITATIONS
SEE PROFILE

Shivaprakash Ramakrishna
ETH Zurich
15 PUBLICATIONS **66** CITATIONS
SEE PROFILE

Prathima Nalam
University of Pennsylvania
17 PUBLICATIONS **135** CITATIONS
SEE PROFILE

Langmuir

Article

pubs.acs.org/Langmuir

Exploring Lubrication Regimes at the Nanoscale: Nanotribological Characterization of Silica and Polymer Brushes in Viscous Solvents

Prathima C. Nalam,† Shivaprakash N. Ramakrishna, Rosa M. Espinosa-Marzal, and Nicholas D. Spencer*

Laboratory for Surface Science and Technology, Department of Materials, ETH Zurich, Wolfgang-Pauli-Strasse 10, 8093 Zurich, Switzerland

Supporting Information

ABSTRACT: Nanotribological properties of silica surfaces, with and without adsorbed, brushlike copolymers of poly(L-lysine)-*graft*-poly(ethylene glycol) (PLL-*g*-PEG) and poly(L-lysine)-*graft*-dextran (PLL-*g*-dextran) have been investigated in aqueous viscous solvent mixtures by means of colloid-probe lateral force microscopy. Lateral forces for PEG/dextran brushes have been measured as a function of shear velocity in aqueous mixtures of glycerol and ethylene glycol (EG), which are highly miscible with water, but are poor solvents for hydrophilic PEG and dextran chains. Prior to the friction measurements on polymer brushes, a nanoscale Stribeck curve was obtained on a bare silica surface in the selected aqueous cosolvent mixtures. The Stribeck curve for bare surfaces indicates the existence of a surface-solvating thin film due to the adsorption of hydrated ions, preventing direct silica−silica contact in the boundary-lubrication regime. A clear transition to the hydrodynamic regime is seen at high speeds for solvents with higher viscosities. The polymer brushes, however, show a shear-thinning effect with increasing shear speed and a combined influence of polymer film and solvent viscosity on the measured friction forces. The formation of an interfacial fluid-film is shown to shift the hydrodynamic regime of hydrated brushes to a lower value of $U\eta$. The correlation between the structural configuration and the corresponding frictional properties of the polymer brushes upon changing solvent quality is discussed.

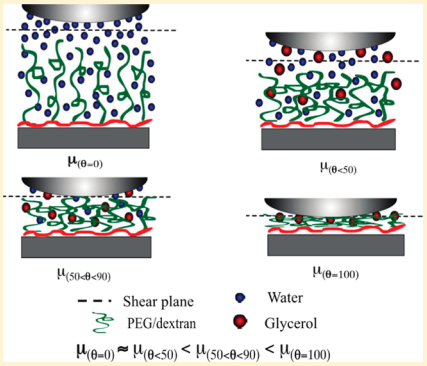

INTRODUCTION

Nature lubricates a wide variety of biological systems in aqueous media, with the help of a few selected biomacromolecules, such as glycoproteins. The macromolecules act as load-bearing elements, enhancing the lubrication properties of water, which would otherwise be poor, due to its low viscosity. Observations of nature's approach to lubricating surfaces have led to the development of brush-assisted aqueous lubrication. Polyelectrolyte copolymers resembling glycoproteins, such as poly(L-lysine)-*graft*-poly(ethylene glycol) (PLL-*g*-PEG)[1,2] and poly(L-lysine)-*graft*-dextran (PLL-*g*-dextran),[3] have been shown to reduce the friction at the contact when adsorbed onto silica surfaces. When such strongly hydrated polymer-coated surfaces are compressed against each other, repulsive steric forces acting between the polymer brushes, osmotic and entropic in origin, maintain the surface separation, while preserving a high fluidity at the brush−brush interface leading to very low friction coefficients.[4−6] Polymer brushes in aqueous solutions have shown friction coefficients as low as 10^{-4} when probed by means of the surface forces apparatus.[7,8]

Extending the application of aqueous-based brush-assisted lubrication across several lubrication regimes is of interest in the development of green lubricants. The viscosity of the lubricant plays an important role in lubricating surfaces and influences the particular lubricating regime in which tribo-pairs operate. One approach to increase the fluid viscosity for water-based, brush-assisted lubrication is the use of aqueous viscous solvent mixtures. In our previous study,[9] aqueous glycerol solutions, which are polar, and viscous in comparison to water, were shown to improve the macrotribological performance of the water-based polymer lubrication system. Polymers in solvent mixtures can combine the advantages of both cosolvents. The presence of water maintains the hydrophilic polymer in a hydrated state and reduces friction at low speeds, while the enhanced bulk viscosity of the solution due to the presence of viscous cosolvent increases the load-bearing capacity of the lubricant. However, at the nanoscale, in the absence of wear, the frictional properties of polymer brushes are influenced by the conformation of the brushes, which is highly affected by the solvent quality. The influence of solvent quality caused by a change in composition of solvent mixture or temperature, on polymer conformations, and hence on the measured friction forces, has been investigated both experimentally[10−12] and by means of computer simulations.[13,14] Granick et al.[15] and others[13] suggest a higher degree of interpenetration of polymer chains in theta or poor solvents, which will lead to higher friction forces in comparison to the behavior in good solvents under relatively similar compressive loads. Apart from the increased width of the overlapping zone in theta and bad

Received: June 6, 2013
Revised: July 15, 2013
Published: July 16, 2013

solvents, the reduced polymer−solvent interaction strength will also lead to a viscous, collapsed, and less lubricious film.[14,16,17]

The conformational transitions of PLL-*g*-PEG brushes were previously studied via the systematic variation of the composition of a binary solvent mixture (isopropanol/water), by employing QCM-D and AFM techniques.[18] Preferential solvation of the PEG brush by the better solvent (water) resulted in a good lubricating film until the volume fraction of the bad cosolvent (isopropanol) in the solution exceeded 85 vol %. On the other hand, the solvation of polymer films such as poly(2-(methacryloyloxy)ethyl phosphorylcholine) (PMPC),[19] poly(*N*-isopropylacrylamide) (PNIPAM),[20] polystyrene (PS),[10] and poly(acrylamide) (PAAm)[21] in mixed alcohol/water solvent mixtures have shown a "co-nonsolvency" effect at a critical concentration of alcohol in the aqueous solvent mixture, accompanied by increased adhesion and friction force, as the brushes undergo a solvent-induced glass transition. In spite of several reports that explored the effect of solvent quality on frictional properties of polymer brushes using solvent mixtures, very few studies have been conducted to describe the effect of solvent viscosity[22] on the tribological properties of polymer brushes, especially at the nanoscale. With the increase in the use of ionic liquids[22−27] and polymer brushes in oil-based solvents[28,29] as lubricants for many micro/nanoengineering applications, it is important to understand the effect of solvent viscosity on the measured friction and adhesion forces.

This paper describes the nanoscale lubrication mechanism of PEG and dextran brushes in viscous, aqueous glycerol and ethylene glycol (EG) solutions, as investigated by colloid-probe lateral force microscopy. The velocity dependence of friction forces is first measured for bare contacts as a function of the solvent viscosity, and a nanoscale Stribeck curve is generated. Different lubrication regimes for bare surfaces are identified. Starting from this basis, the influence of the adsorbed polymer brushes on the measured friction was determined at different shear speeds in the same solvent mixtures. Also, the observed tribological behavior of PEG and dextran brushes as a function of solvent quality is correlated with conformation changes, as studied in one of our previous works using the quartz crystal microbalance.[30]

MATERIALS AND METHODS

Solvent Mixtures. Aqueous solutions of glycerol (ABCR GmbH, Karlsruhe, Germany) and ethylene glycol (Sigma Aldrich) with HEPES buffer [10 mM of 4-(2-hydroxyethyl)-1-piperazine-1-ethanesulfonic acid (Sigma, St. Louis, MO), pH = 7.4] were freshly prepared prior to each experiment. Selected solvent mixtures used in this study and their corresponding viscosity values are given in Table 1.

Preparation of Surfaces. The polyelectrolyte copolymers, PLL(20 kDa)-*g*[3.6]-PEG(5 kDa) and PLL(20 kDa)-*g*[3.5]-dextran(5 kDa) (*g* = grafting density) were purchased from SuSoS AG (Dübendorf, Switzerland). The copolymers can form brushlike structures when adsorbed onto negatively charged substrates via electrostatic adsorption.[3,33] Prior to adsorption, the silicon wafers were sonicated in ethanol for 30 min and were then glued to Petri dishes (ϕ = 30 mm, TPP, Switzerland) using an UV-curable glue (NOA 63, Norland Optical Adhesive, Cranbury, NJ), to avoid flotation of samples when immersed in the aqueous mixtures. After curing, the samples were UV-ozone treated (UV clean, Boekel Industries Inc., Feasterville-Trevose, PA) for 40 min to remove any organic contamination. The adsorption of polymer on silica wafers from HEPES buffer was carried out at a concentration of 0.25 mg/mL for 45 min. After adsorption, the samples were rinsed in copious amounts of Milli-Q water to remove any physisorbed polymer from the surface. The samples were dried in a stream of nitrogen gas and were immersed in the selected solvent mixture before being placed in the AFM.

Table 1. Solvent Mixtures Used in This Study and Their Corresponding Viscosities

vol % of glycerol in HEPES	viscosity (mPa·s)[31]	vol % of ethylene glycol in HEPES	viscosity (mPa·s)[32]
0	0.89	0	0.89
25	2.15	25	1.76
50	6.80	50	3.54
75	41.20	75	7.24
100	945	100	17.01

Friction and Adhesion Force Measurements by Colloidal-Probe Atomic Force Microscopy. Friction measurements were carried out with an atomic force microscope (MFP-3D, Asylum Research, Santa Barbara, CA). Lateral force measurements were performed with a bare silica colloid probe against a bare (naturally oxidized) or polymer-functionalized silicon surface in different solvent mixtures. Tipless, gold-coated cantilevers (CSC12, MikroMasch, Estonia) with a normal stiffness of 0.5−0.7 N/m were used to measure lateral forces. Silica microspheres (EKA Chemicals AM, Kormasil) with diameters ranging from 15 to 20 μm were attached to the tipless cantilever using UV-glue (NOA 63, Norland Optical Adhesive, Cranbury, NJ). The colloid-modified AFM cantilever was UV-ozone treated for 30 min prior to use. The solvent mixture in the Petri dish was manually exchanged prior to each experiment after copious rinsing of the sample with Milli-Q water and drying in a stream of nitrogen gas. Sliding velocities between 0.5 and 500 μm/s were obtained by varying the stroke length and the scan frequency of the friction loop. The postanalysis of the measured lateral forces was conducted by means of IGOR Pro 6.2 software, and the average friction loop width was determined.

Pull-off measurements were conducted using cantilevers with preattached silica colloids (Novascan Technologies, Ames, IA). Around 36 force−distance curves were acquired over a scan area of 20 × 20 μm^2 on bare (naturally oxidized) silicon and polymer-functionalized surfaces immersed in the selected aqueous glycerol and EG mixtures. Interpretation of the measured force curves needs to take into account the contribution of viscous forces originating from the surrounding viscous solvent mixtures. These viscous forces scale as a function of contact radius and the approach speed of the colloidal probe. Thus, the force curves were first obtained for nonadhesive bare silica surfaces in pure glycerol and EG solutions at different approach speeds varying from 2 μm/s down to 100 nm/s. At high tip velocities, in pure glycerol, high repulsive forces during approach and high pull-off forces during retraction were observed due to hydrodynamic drag forces experienced by the tip in viscous solvents.[34] However, the force curves obtained at slower approach speeds, that is, 100 nm/s for glycerol and 200 nm/s for EG solutions using an AFM cantilever with normal stiffness = 4.5 N/m and colloid diameter = 5 μm, showed no influence of viscous forces on the measured adhesion forces and thus these conditions were selected to measure the adhesion forces between polymer brushes and the colloidal sphere in all the selected solvent mixtures. The mean and standard deviation of the measured pull-off forces were estimated by fitting a Gaussian function to the obtained histograms. The force measurements were made under complete immersion of tip and sample in the solvent, to avoid capillary effects.

The normal and lateral signals, measured using AFM, were converted to forces using appropriate calibration constants. The normal spring constant calibration of the cantilever was carried out using the thermal-noise method[35] before the attachment of the colloidal probe. The torsional spring constant was estimated using Sader's method[36] with the help of Sader's online calibration applet. The lateral sensitivity (S_L) for the cantilever (probe-cantilever) was estimated using the test-probe method, as described by Cannara et al.[37] for rectangular cantilevers. Here, a silicon wafer was cut along the ⟨100⟩ crystal plane and was glued to a glass slide, such that the smooth edge of the silicon wafer was used as a wall to twist the cantilever

dx.doi.org/10.1021/la402148b | *Langmuir* 2013, 29, 10149−10158

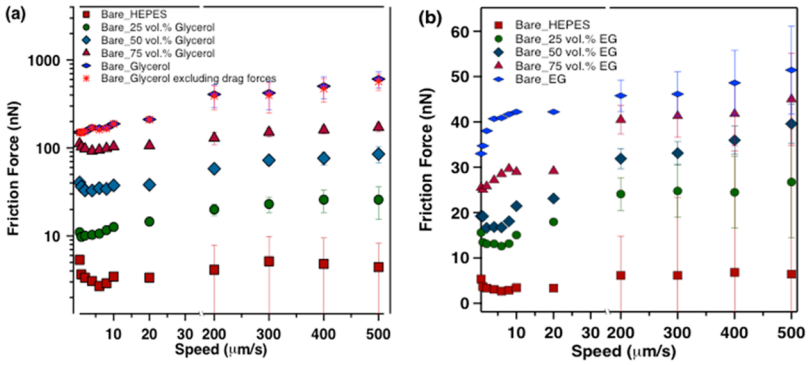

Figure 1. Speed dependence of friction forces measured between a bare silica colloid against naturally oxidized silicon surface in aqueous solutions of glycerol (a) and EG (b). The effect of drag forces on the AFM cantilever, when scanned laterally in highly viscous solvents such as glycerol, is shown to be negligible, i.e., the blue flat diamonds overlap the red crosses. All measurements were conducted at a constant normal load of 100 nN.

laterally. A test-cantilever modified with a colloidal sphere (with sphere diameter larger than the width of the cantilever) was twisted against the silicon wall and the lateral sensitivity, estimated from the slope of lateral deflection plotted vs piezo distance, was measured for all the solvent mixtures. The lateral sensitivity of the target cantilever was estimated from the measured lateral sensitivity of the test cantilever as described in detail in ref 37.

RESULTS AND DISCUSSION

Lateral forces were measured using a bare silica colloid against a naturally oxidized silicon surface or polymer-grafted surface (asymmetric contact), in aqueous mixtures of glycerol and EG. The maximum contact pressures between the silica probe (diameter = 15 μm) against a flat silica surface, in the absence of adhesion, can be obtained using the Hertz equation.[38] For a normal load of 100 nN, E_{silica} = 72 GPa and ν_{silica} = 0.17, a contact pressure of 120 MPa is obtained. However, upon adsorption of polymer film, the moduli of the polymer films are known to vary between ≈150 and 700 kPa[20,39] resulting in contact pressures being reduced to around 20 and 60 kPa. At such low contact pressures, the wear of the polymer by the colloid probe can be neglected. Also, the load-dependent friction-force measurements for polymer brushes (not shown) show no hysteresis in the friction forces measured upon increasing and decreasing the load up to 200 nN, indicating the absence of wear of the polymer film and of the counter-surface in the contact.[40]

Velocity-Dependent Studies for Bare−Bare Silica Contacts in Viscous, Aqueous Solvent Mixtures. Figure 1 shows the friction force, measured at a normal load of 100 nN, plotted against sliding speed for a bare colloid against a bare silica surface with increase in glycerol (a)/EG (b) volume percentage in HEPES solution. An initial decrease in friction force was observed with increase in shear speed up to 5 μm/s, beyond which the friction force increases in aqueous solutions of glycerol and EG. This initial decrease in friction was also observed by Donose et al.[41] for bare silica contacts in pure water and ionic aqueous solutions and ascribed to the shortened contact time at the interface, such that the degree of disruption of the adsorbed layer of water or hydrated ions onto the surface decreases. This transition, however, was not observed for contacts in pure glycerol or EG, which show a continuous increase in the friction force from the lowest measured shear speeds.

Lateral movement of a cantilever in highly viscous solvents, such as 100% glycerol, can induce lateral drag forces on the cantilever. In order to estimate and then eliminate the contribution of such drag forces from the obtained lateral signal, the cantilever was scanned in pure glycerol without coming into contact with the silica substrate (at zero applied load) as a function of speed. The obtained drag forces as a function of speed were subtracted from the friction forces obtained in pure glycerol (red crosses). Drag forces are found to have a negligible influence on the measured friction forces (overlap of blue flat diamonds and red crosses) and hence can be neglected.

Figure 2 shows friction forces measured between silica−silica contacts as a function of applied normal load at low sliding

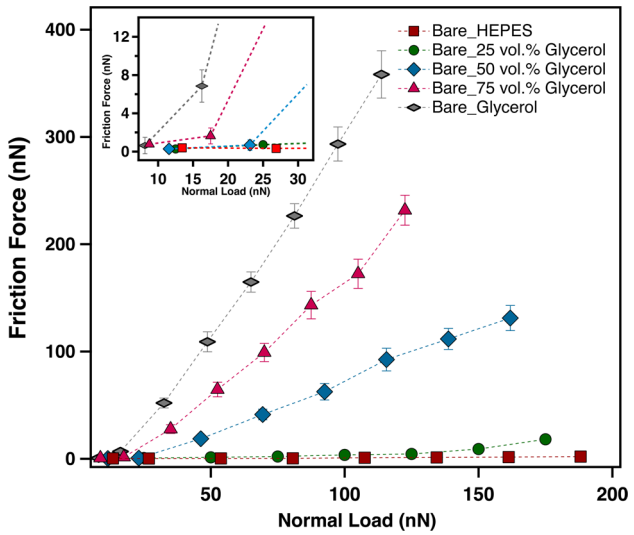

Figure 2. Friction force as a function of normal load measured using a bare silica colloid against a naturally oxidized silicon surface in aqueous glycerol mixtures at a shear speed of 1 μm/s. The inset shows the magnitude of friction forces at extremely small normal loads.

speed (1 μm/s) in aqueous glycerol solutions. An Amonton's-law-like dependence of friction forces is observed for all concentrations of glycerol, except at extremely low loads (below 30 nN), where the coefficients of friction were found to be an order lower than the friction coefficients obtained at higher normal loads, irrespective of the composition of the solvent mixtures at the contact (inset in Figure 2). The onset of increase in friction force occurs at lower normal loads with increasing glycerol content in the solvent mixture.

Figure 3 shows a nanoscale Stribeck curve (obtained from Figure 1), in which the coefficient of friction (COF, μ) (ratio of

dx.doi.org/10.1021/la402148b | Langmuir 2013, 29, 10149−10158

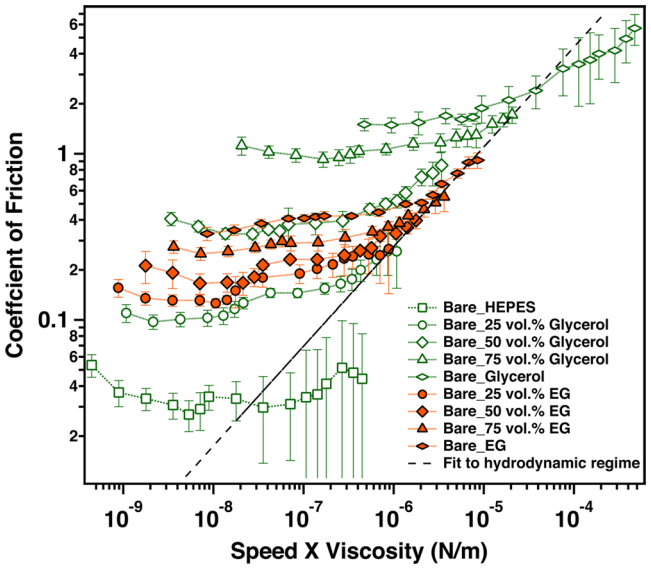

Figure 3. Dependence of coefficient of friction on speed multiplied by viscosity ($U\eta$). Nanoscale Stribeck curve obtained for a silica colloidal probe sliding on a bare silica surface at a constant normal load of 100 nN for aqueous–glycerol mixtures (open green) and aqueous–EG mixtures (filled orange). A simple power-law line is plotted to differentiate the hydrodynamic regime from the boundary regime at the nanoscale.

friction force to normal load) is plotted against shear speed (U in m/s) multiplied by the viscosity of the aqueous solvent mixture (η in N·s/m^2), for a bare silica colloid when slid against the bare silicon (naturally oxidized) surface at a constant normal load of 100 nN. The shape of the Stribeck curve obtained for bare contacts as a function of glycerol or EG concentration in aqueous solutions at the nanoscale (Figure 3) is significantly different from that obtained at the macroscale.[9] The measured friction coefficients do not overlap at low $U\eta$ values (boundary lubrication regime), but instead a vertical offset in friction coefficient was observed upon increasing glycerol or EG percentage at the contact. However, at higher $U\eta$ values, hydrodynamic lift-off forces set in and the coefficient of friction values for different solvent mixtures are seen to converge, except for pure HEPES and glycerol. The low pressure-viscosity coefficient of HEPES solutions maintains the viscosity of the lubricating film constant and shifts the onset of the hydrodynamic regime to inaccessible speeds. In the measurements with pure glycerol, high errors bars were obtained, indicating an instability of the cantilever at high velocities in the highly viscous liquid.

A simple empirical power law, as described by Bongaerts et al. for macroscopic systems,[42] is applied to predict the friction coefficient of the surfaces in the hydrodynamic regime at the nanoscale.

$$\mu = k(U\eta)^n \quad (1)$$

where k and n are constants. n describes the flow properties of the confined film under shear, and k accounts for the material properties of the interface. A good fit at high $U\eta$ is obtained with k = 0.11 and n = 0.6, which are close to the values obtained in ref 42 using similar solvent mixtures, indicating the presence of the hydrodynamic regime at the nanoscale (Figure 3).

At low $U\eta$ values, in Figure 3, and above the transition load (30 nN), as indicated in Figure 2, the friction coefficient is seen to increase upon increasing the glycerol percentage. Increase in nonhydrodynamic friction forces in the silica–silica contact as a function of solvent composition suggests the existence of an interfacial film, either due to different chemical interactions of the two solvent molecules with the silica substrate or due to the formation of a physically adsorbed film by the polar solvents at the interface. A similar increase in friction coefficient was also observed when a silica sphere was slid against a freshly cleaved mica surface in similar solvent mixtures (not shown), consistent with the absence of any chemically induced film-formation with the underlying silica substrate for a given solvent mixture.

The adsorption of hydrated cations on hydrophilic mica[43,44] has been shown to increase the short-range hydration repulsion forces, thus influencing the lubrication properties.[45] Silica surfaces,[41] also, in the presence of ions, especially small, strongly hydrated ions such as K^+ or Li^+, have been shown to lower shear forces, in comparison to larger, poorly hydrated ions such as Cs^+. Silica surfaces additionally have shown "intrinsic" hydration forces even at extremely low or zero concentrations of counterions.[46,47] Several possible mechanisms, such as polarization of water by surface dipoles, physical adsorption of hydrated counterions, or hydrogen bonding of the solvent molecules with the surface groups, can act together to increase the short-range repulsive forces near charged surfaces. The plane of charge is farther away from the surface for silica than for mica, due to the formation of silicic acid groups in aqueous media,[48] and the formation of hydrogen bonds with silanol groups (Si–OH) by neighboring water molecules/ions is likely to play an important role in silica hydration.[49] Hence, the change in friction coefficient as a function of glycerol concentration in the boundary-lubrication regime (Figure 3) is influenced by the reduced hydrogen bonding ability of glycerol/EG molecules with the silanol groups, in comparison to water molecules or hydrated HEPES ions. The strong enthalpic interaction between glycerol or EG[50,51] and bulk water molecules, together with the larger size of glycerol/EG molecules,[52] may reduce the hydrogen-bonding interactions with the silanol groups. Thus, as the percentage of glycerol at the interface is increased, the concentration of hydrated HEPES ions at the interface decreases and the friction forces are enhanced, owing to the reduction in repulsive hydration forces.

At contact loads below the transition load in Figure 2, the steric-hydration forces due to adsorbed hydrated ions keep the surfaces apart. As the percentage of glycerol increases, the reduced concentration of hydrated ions shifts the transition load to lower loads (Figure 2 inset). However, even in pure glycerol, a small amount of steric-solvation repulsion is observed, indicating a probable formation of a thin solvating film by the glycerol molecules with the silanol groups.[52] As the applied load increases, the repulsive hydration forces are overcome and the adsorbed hydrated ions at the interface are sheared away from the contact, increasing the friction forces[45] (Figure 2). The increase in frictional forces in different solvent mixtures as a function of load depends on the strength of interfacial interactions by the solvent molecules with the underlying surface. Upon further increase in load, such as during macroscale measurements, the interactions between solvent molecules and the substrate become less significant, in the presence of wear, and the coefficients of friction for all

dx.doi.org/10.1021/la402148b | Langmuir 2013, 29, 10149–10158

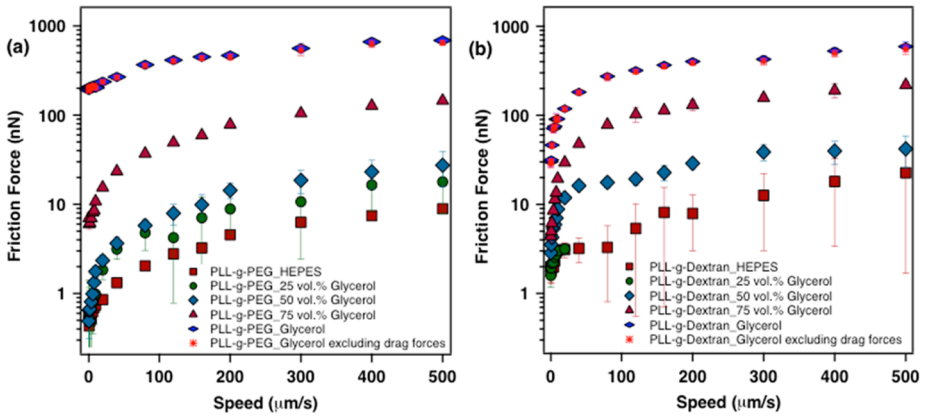

Figure 4. Dependence of friction force on shear speed for (a) PEG- and (b) dextran-coated surfaces in aqueous glycerol solutions at a constant normal load of 100 nN.

solvent mixtures, within a given lubrication regime, merge to a single value.

Velocity-Dependence Studies of Polymer-Coated Silica Surfaces in Viscous, Aqueous Solvent Mixtures. Figure 4 shows a sublinear increase in friction forces with shear speed for PEG (a) and dextran (b) coated surfaces in aqueous glycerol solutions measured at a normal load of 100 nN. No initial decrease in friction with speed, as observed for the bare surface in most cases (Figure 1), was observed for polymer brushes. However, an increase in friction force with increase in cosolvent concentration in the aqueous solution is observed for both brushes. Similar trends were observed for PEG- and dextran-coated surfaces in aqueous-EG solutions (not shown). It is important to note that polymer brushes with $L/2R_g$ (where L is the mean spacing between the neighboring chains and R_g is the radius of gyration of the PEG or dextran in bulk) lower than 0.5 have a transition load, the load at which the brush compression and brush parting/interdigitation are in equilibrium, above 100 nN (0.16 MPa for $d_{colloid}$ = 5 μm).[53] PEG[33] and dextran[3] brushes with the architectures specified in this study have $L/2R_g \sim 0.45$ in pure HEPES, and thus, for a compressive load of 100 nN (0.05 MPa for $d_{colloid}$ = 15 μm), the brushes are below the transition load and at a constant speed of 1 μm/s[53] there still exists an interfacial fluid film between the colloid probe and the brush. Values for R_g in the solvent mixtures are unknown.

The sublinear increase in friction force for polymer brushes in solvent mixtures can be described by the stretching of chains in the sliding direction, under shear. For brushes in a good solvent, Grest[54] and many others have shown, using simulations,[55−57] that at smaller shear velocities less or no tilting of polymer chains (estimated by radius of gyration R_g) is observed and thus friction forces increase approximately linearly with velocity (Newtonian-type behavior). However, higher shear rates, as the brushes start to stretch and tilt away from the penetration zone, lead to a reduction in brush−brush (for symmetric contact) or brush−countersurface (for asymmetric contact) interactions. Klein et al.[58] related the tilting and stretching of the polymer chains upon sliding to an increase in osmotic repulsion and thus to an increase in the gap distance, and consequently to a decrease in the effective viscosity of the film between the two surfaces (polymer and fluid). This would explain the observed shear thinning and the sublinear increase in friction with sliding velocity. Upon increasing the cosolvent concentration, the lower solvent quality results in a gradual decrease in the swelling ratio of the brushes. Thus, under similar compressive load, the resistance of the brushes to stretching leads to an increase in friction force at a given speed and shear thinning sets in at higher shear rates than at lower cosolvent concentrations.

Figure 5 compares the $U\eta$ dependence of friction force for a bare silica surface (from Figure 3) with results for PEG-coated and dextran-coated surfaces in selected aqueous−glycerol mixtures. A similar plot for aqueous ethylene glycol solutions is shown in the Supporting Information (S1). For the polymer-brush-coated surfaces, unlike the case of bare surfaces, a gradual increase in friction force is observed with increase in $U\eta$. The presence of polymer brushes leads to a significant reduction in friction forces in comparison to bare surfaces in almost all solvent mixtures. At low values of $U\eta$, corresponding to the boundary−lubrication regime for bare contacts, a 1−2 orders of magnitude reduction in friction force is observed for the polymer-coated surfaces. At higher values of $U\eta$, in the hydrodynamic regime for bare contacts, where the surfaces

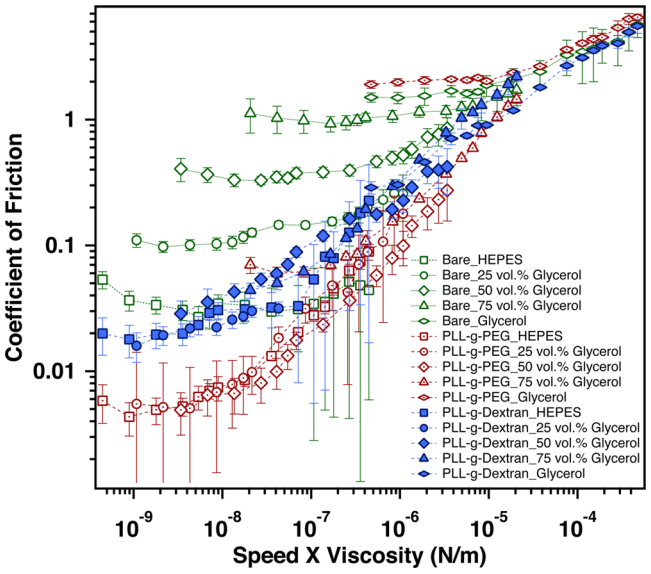

Figure 5. Dependence of coefficient of friction (COF) on speed multiplied by viscosity ($U\eta$) for bare silica (open green), PEG- (open-dot-red), and dextran (filled blue)-coated surfaces at a normal load of 100 nN in aqueous−glycerol solutions.

dx.doi.org/10.1021/la402148b | Langmuir 2013, 29, 10149−10158

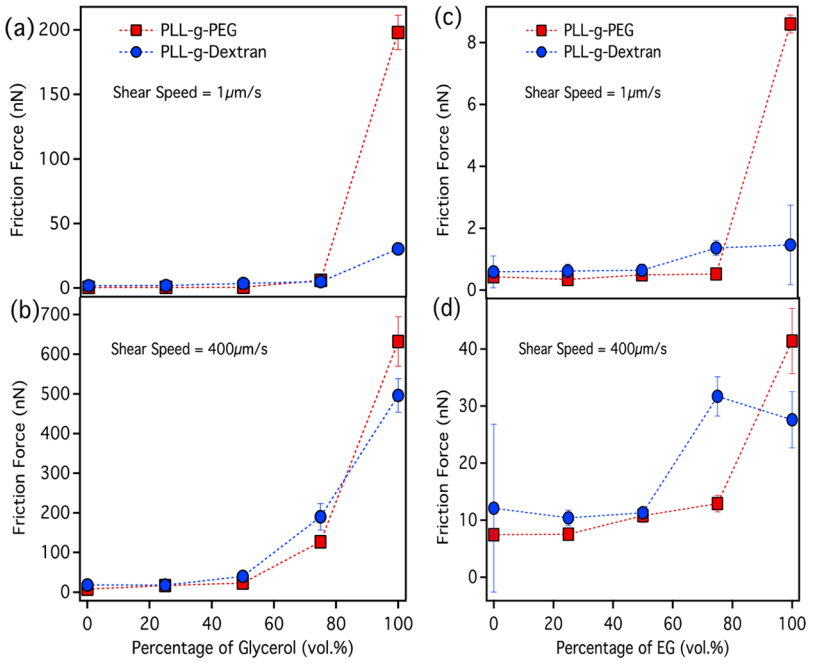

Figure 6. Friction forces as a function of volume percentage of cosolvent: (a) at 1 μm/s and (b) at 400 μm/s for aqueous−glycerol mixtures; and (c) at 1 μm/s and (d) at 400 μm/s for aqueous−EG mixtures.

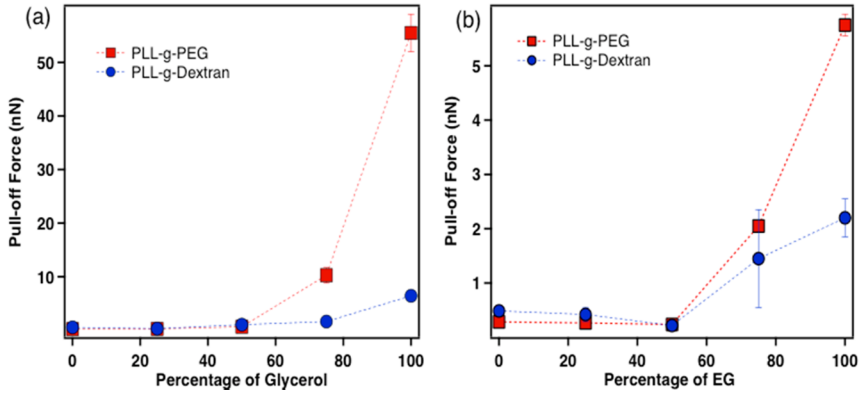

Figure 7. Pull-off forces as a function of volume percentage of glycerol (a) and EG (b) in HEPES for PEG- and dextran-coated surfaces. The mean and standard deviations of the pull-off forces are obtained by fitting Gaussian functions to the measured histograms. Note that the *y*-axes have different scales for (a) and (b).

are separated by means of hydrodynamic lift-off, the influence of the polymer brushes on the resultant friction force is still remarkable: a 20−30% reduction in friction force is observed in presence of polymer brushes, with the exception of PEG brushes in pure glycerol.

The formation of an interfacial fluid film owing to the repulsion between the hydrated brushes and the counter-surface shifts the hydrodynamic regime to lower $U\eta$, in comparison to the behavior of bare contacts. The brush-induced hydrodynamic regime is influenced by both the effective viscosity of the polymer film and the viscosity of the interfacial fluid film. Increasing speed leads to a brush-tilting and shear-thinning effect, as discussed above. At sufficiently high $U\eta$, due to hydrodynamic lift-off, the viscosity of the solvent mixture dominates the interfacial friction and the curves come closer to the Stribeck curve for the bare surface.

At low $U\eta$, the polymer conformation influences the measured friction forces through its effective viscosity: with decrease in solvent quality, the polymer brushes become less solvated and gradually collapse, resulting in deviations from the hydrodynamic regime. PEG brushes in 75 vol % glycerol and in pure glycerol show an order of magnitude vertical offset in the COF at low $U\eta$ (red pyramids and diamonds). Their speed-independent frictional behavior at low $U\eta$ points to a boundary-like regime for brushes in these solvent mixtures. Due to the better solubility of dextran in glycerol, the vertical offset of the coefficient of friction is not observed for dextran brushes (Figure 5). Also in EG mixtures, owing to the better solvent quality for both PEG and dextran brushes, the boundary-like regime is less pronounced (see Supporting Information S1).

Influence of Structural Properties of Polymer Brushes on Tribological Properties in Aqueous−Viscous Solvent Mixtures. Figure 6 shows friction forces for PEG and dextran brushes at two different shear speeds, 1 μm/s (low speed) and 400 μm/s (high speed), at different volume percentages of glycerol (a, b) and EG (c, d) in aqueous solution. The friction forces as a function of solvent composition for both the polymer brushes show negligible variation in friction force up

dx.doi.org/10.1021/la402148b | *Langmuir* 2013, 29, 10149−10158

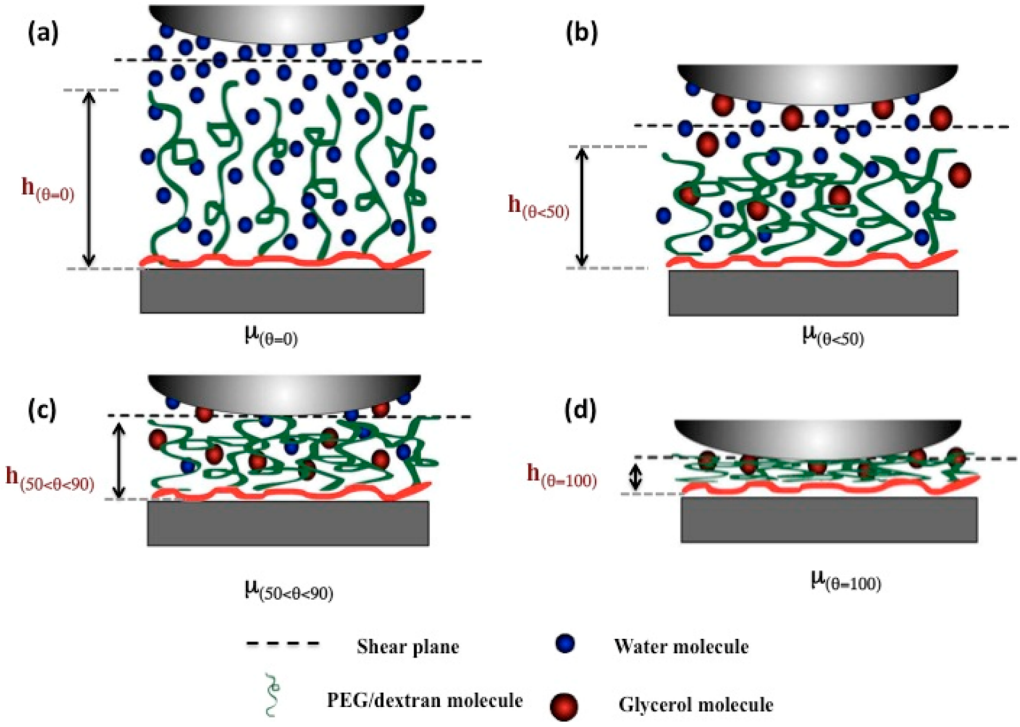

Figure 8. Schematic representation of conformation of polymer brushes in aqueous solvent mixtures under shear. The shift in the shear plane with reduction in solvent quality is shown.

to 50−75 vol % of both glycerol/EG in the solvent mixture at all tested sliding speeds. Beyond this critical concentration, an abrupt increase in friction force is observed. Also, the PEG-functionalized surfaces show lower friction coefficients at all cosolvent percentages than dextran-functionalized surfaces (also see Figure 5), except for the case of pure glycerol, in spite of the generally better solubility of the dextran monomer in aqueous−glycerol solutions. Dextran brushes, due to the higher persistent length of the dextran chains, are more rigid polymers. Quartz crystal microbalance measurements (QCM)[30] have shown higher shear moduli for dextran brushes in comparison to PEG brushes in similar aqueous solvent mixtures. Thus the increase in rigidity or stiffness may explain the increase in friction owing to the increasing effective viscosity of the film between the sliding surfaces. The effect of solvent quality on friction is observed only when the PEG brushes are strongly collapsed, leading to higher friction forces for PEG in pure glycerol or ethylene glycol, in comparison to dextran.

Similar trends were also observed for the adhesion forces measured between polymer brushes and the silica colloidal sphere in the selected aqueous solvent mixtures (Figure 7). As indicated in the Materials and Methods section, the influence of hydrodynamic drag was avoided by selecting slow approach and separation speeds (100 nm/s in glycerol and 200 nm/s in EG). The average pull-off force measured for PEG- and dextran-coated surfaces as a function of volume concentration of glycerol (Figure 7a) and EG (Figure 7b) in HEPES shows negligible variation up to 50−75 vol % of the cosolvent; however, beyond this critical concentration, the measured pull-off forces between PEG/dextran brushes and the bare colloid tip abruptly increase. The measured pull-off forces for dextran brushes were slightly higher than those for the PEG brushes at low concentrations of cosolvent and above 50 vol % cosolvent concentrations, the PEG brushes showed higher adhesion than the dextran brushes, in agreement with the friction results.

In our previous communication,[30] the conformational properties of PEG and dextran brushes were studied in mixtures of water (good solvent) and glycerol/EG (poor solvent) by means of QCM. PEG films show a 40% collapse in thickness even at 45 vol % of glycerol and 75 vol % of EG in aqueous solution. Dextran brushes also show a collapse in film thickness but to a lesser extent due to the better solvent quality of the selected solvent mixtures for dextran, that is, about 15−25% collapse in thickness for a similar increase in volume concentration of glycerol and EG. A solvent-quality-induced brush collapse will result in a significant increase in the pull-off force, which can be explained by additional physical bonds between the tip and the collapsed polymer chains (Figure 7) and the increased adhesion directly relates to the measured friction forces (Figure 6).

The collapse of polymer brushes with decreasing solvent quality is seen to affect the obtained frictional forces, but not in a similar fashion. While no significant increase in the frictional forces, and in adhesion, for PEG and dextran brushes is observed below 50 vol % of cosolvent, an abrupt increase of both friction and adhesion is observed beyond this critical concentration. However, both the brushes show a continuous (linear) collapse with increase in volume percentage of poor solvent.[30] In contrast, the results obtained by Müller et al.[18] showed a direct correlation between the polymer conformations and the obtained friction forces with a transition volume concentration of 85 vol % of isopropanol in aqueous buffer. The reason for the different results is to be found in the free energy of mixing between water and the cosolvent. While the continuous collapse of the polymer brushes for aqueous−glycerol/EG mixtures at low concentrations of the cosolvent was ascribed to the high enthalpic interaction between the

dx.doi.org/10.1021/la402148b | *Langmuir* 2013, 29, 10149−10158

cosolvents, a cosolvent separation in aqueous isopropanol mixtures is possible due to the low free energy of mixing.[30]

The different trends observed for conformation changes and frictional forces for polymer brushes emphasize the effect of the interfacial fluid film on the obtained friction forces. The interfacial fluid layer acts as the shear plane (Figure 8a,b) between the polymer brush and the colloid probe up to a critical concentration of the cosolvent, in our case up to 50−75 vol % of cosolvent (Figure 8b), in spite of the significant brush collapse, and thus can explain the lower friction forces. However as the concentration of the cosolvent with poor solvent quality is further increased, the brushes undergo significant collapse, and the fluid film at the interface can no longer be maintained. The shear plane now exists at the interface of the polymer film and the colloid probe, resulting in higher friction coefficients either due to entanglement of the brushes adsorbed onto opposite surfaces or due to continuous bond-forming and separation between the polymer and the bare colloid probe (Figure 8c, d).

CONCLUSIONS

The frictional response of PEG and dextran brushes as a function of the solvent quality in aqueous solutions of glycerol and EG has been measured by means of colloidal-probe lateral force microscopy. The effect of solvent viscosity on the measured friction forces was characterized by plotting a *nanoscale* Stribeck curve for bare silica surfaces. The polymer-coated surfaces in viscous, aqueous, solvent mixtures show a reduction in friction force at all values of $U\eta$ except for brushes in very poor solvents. The presence of an interfacial fluid film for solvated polymer brushes shifts the hydrodynamic lubrication regime to smaller values of $U\eta$. The friction forces for brush-coated surfaces are seen to be influenced by both effective viscosity of the polymer film (more at lower $U\eta$) and viscosity of the interfacial film (more at higher $U\eta$). PEG brushes show lower friction forces in comparison to dextran brushes in almost all solvent mixtures, except in pure glycerol/EG. Thus, despite the better solubility of dextran brushes (in comparison to PEG brushes) in the selected solvent mixtures, the reduction of dissipative forces due to better solvation could not overcome the increase of the dissipative forces due to the higher stiffness of the dextran brushes. Thus, the stiffness of the polymer brushes, in comparison to polymer−solvent interactions, is seen to play a more important role in the dissipation mechanism of the studied brushes. Also, the presence of the interfacial fluid-film layer is seen to delay the increase in friction forces, despite a continuous collapse of the polymer film with an increase in volume percentage of the poor solvent in the solvent mixture. Thus, a direct correlation between the polymer conformation and the measured friction or adhesion forces is not always going to be present, since the fluid-film properties appear to dominate the system. Understanding the regimes in polymer-brush lubrication as a function of polymer properties, polymer−solvent interactions, and solvent viscosity will facilitate the application of polymer films as lubricants in many potential micro/nanoscale engineering applications.

ASSOCIATED CONTENT

Supporting Information

Friction forces for bare silica and polymer-adsorbed surfaces with varying viscosity of aqueous EG mixtures. This material is available free of charge via the Internet at http://pubs.acs.org.

AUTHOR INFORMATION

Corresponding Author

*E-mail: nspencer@ethz.ch.

Present Address

[†]P.C.N.: Department of Mechanical Engineering and Applied Mechanics, University of Pennsylvania, 112 Towne Building, Philadelphia, PA, 19104, USA.

Author Contributions

The manuscript was written through contributions of all authors. All authors have given approval to the final version of the manuscript.

Notes

The authors declare no competing financial interest.

ACKNOWLEDGMENTS

The financial assistance of the European Science Foundation, within the Eurocores (FANAS) program is gratefully acknowledged. We would also like to thank Prof. Robert Carpick, Dr. Lucy Clashom, Dr. Jarred Clashom, and Dr. Ang Li for discussions and their valuable suggestions.

REFERENCES

(1) Yan, X. P.; Perry, S. S.; Spencer, N. D.; Pasche, S.; De Paul, S. M.; Textor, M.; Lim, M. S. Reduction of friction at oxide interfaces upon polymer adsorption from aqueous solutions. *Langmuir* **2004**, *20* (2), 423−428.

(2) Lee, S.; Muller, M.; Ratoi-Salagean, M.; Voros, J.; Pasche, S.; De Paul, S. M.; Spikes, H. A.; Textor, M.; Spencer, N. D. Boundary lubrication of oxide surfaces by Poly(L-lysine)-*g*-poly(ethylene glycol) (PLL-*g*-PEG) in aqueous media. *Tribol. Lett.* **2003**, *15* (3), 231−239.

(3) Perrino, C.; Lee, S.; Spencer, N. D. End-grafted Sugar Chains as Aqueous Lubricant Additives: Synthesis and Macrotribological Tests of Poly(L-lysine)-*graft*-Dextran (PLL-*g*-dex) Copolymers. *Tribol. Lett.* **2009**, *33* (2), 83−96.

(4) Grest, G. S. Normal and shear forces between polymer brushes. *Polym. Confined Environ.* **1999**, *138*, 149−183.

(5) Klein, J. Shear, friction, and lubrication forces between polymer-bearing surfaces. *Annu. Rev. Mater. Sci.* **1996**, *26*, 581−612.

(6) Briscoe, W. H.; Titmuss, S.; Tiberg, F.; Thomas, R. K.; McGillivray, D. J.; Klein, J. Boundary lubrication under water. *Nature* **2006**, *444* (7116), 191−194.

(7) Chen, M.; Briscoe, W. H.; Armes, S. P.; Klein, J. Lubrication at Physiological Pressures by Polyzwitterionic Brushes. *Science* **2009**, *323* (5922), 1698−1701.

(8) Klein, J.; Kumacheva, E.; Mahalu, D.; Perahia, D.; Fetters, L. J. Reduction of Frictional Forces between Solid-Surfaces Bearing Polymer Brushes. *Nature* **1994**, *370* (6491), 634−636.

(9) Nalam, P. C.; Clasohm, J. N.; Mashaghi, A.; Spencer, N. D. Macrotribological Studies of Poly(L-lysine)-graft-Poly(ethylene glycol) in Aqueous Glycerol Mixtures. *Tribol. Lett.* **2010**, *37* (3), 541−552.

(10) Nomura, A.; Okayasu, K.; Ohno, K.; Fukuda, T.; Tsujii, Y. Lubrication Mechanism of Concentrated Polymer Brushes in Solvents: Effect of Solvent Quality and Thereby Swelling State. *Macromolecules* **2011**, *44* (12), 5013−5019.

(11) Forster, A. M.; Kilbey, S. M. Effect of solvent quality on the friction forces between polymer brushes. Materials Research Society Symposium Proceedings: *Polym. Interfaces Thin Films***2002***710*179184

(12) Limpoco, F. T.; Advincula, R. C.; Perry, S. S. Solvent dependent friction force response of polystyrene brushes prepared by surface initiated polymerization. *Langmuir* **2007**, *23* (24), 12196−12201.

(13) Yin, F.; Bedrov, D.; Smith, G. D. A molecular simulation study of the structure and tribology of polymer brushes: Comparison of behavior in theta and good solvents. *Eur. Polym. J.* **2008**, *44* (11), 3670−3675.

(14) Kreer, T.; Muser, M. H.; Binder, K.; Klein, J. Frictional drag mechanisms between polymer-bearing surfaces. *Langmuir* **2001**, *17* (25), 7804−7813.
(15) Dhinojwala, A.; Cai, L.; Granick, S. Critique of the friction coefficient concept for wet (lubricated) sliding. *Langmuir* **1996**, *12* (19), 4537−4542.
(16) Schorr, P. A.; Kwan, T. C. B.; Kilbey, S. M.; Shaqfeh, E. S. G.; Tirrell, M. Shear forces between tethered polymer chains as a function of compression, sliding velocity, and solvent quality. *Macromolecules* **2003**, *36* (2), 389−398.
(17) Kitano, K.; Inoue, Y.; Matsuno, R.; Takai, M.; Ishihara, K. Nanoscale evaluation of lubricity on well-defined polymer brush surfaces using QCM-D and AFM. *Colloids Surf., B* **2009**, *74* (1), 350−357.
(18) Müller, M. T.; Yan, X. P.; Lee, S. W.; Perry, S. S.; Spencer, N. D. Preferential solvation and its effect on the lubrication properties of a surface-bound, brushlike copolymer. *Macromolecules* **2005**, *38* (9), 3861−3866.
(19) Zhang, Z. Y.; Morse, A. J.; Armes, S. P.; Lewis, A. L.; Geoghegan, M.; Leggett, G. J. Effect of Brush Thickness and Solvent Composition on the Friction Force Response of Poly(2-(methacryloyloxy)ethylphosphorylcholine) Brushes. *Langmuir* **2011**, *27* (6), 2514−2521.
(20) Sui, X. F.; Chen, Q.; Hempenius, M. A.; Vancso, G. J. Probing the Collapse Dynamics of Poly(*N*-isopropylacrylamide) Brushes by AFM: Effects of Co-nonsolvency and Grafting Densities. *Small* **2011**, *7* (10), 1440−1447.
(21) Li, A.; Ramakrishna, S. N.; Kooij, E. S.; Espinosa-Marzal, M. R.; Spencer, N. D. Poly(acrylamide) films at the solvent-induced glass transition: adhesion, tribology, and the influence of crosslinking. *Soft Matter* **2012**, *8*, 9092−9100.
(22) Nomura, A.; Ohno, K.; Fukuda, T.; Sato, T.; Tsujii, Y. Lubrication mechanism of concentrated polymer brushes in solvents: effect of solvent viscosity. *Polymer Chemistry* **2012**, *3* (1), 148−153.
(23) Perkin, S.; Albrecht, T.; Klein, J. Layering and shear properties of an ionic liquid, 1-ethyl-3-methylimidazolium ethylsulfate, confined to nano-films between mica surfaces. *Phys. Chem. Chem. Phys.* **2010**, *12* (6), 1243−1247.
(24) Ishikawa, T.; Kobayashi, M.; Takahara, A. Macroscopic Frictional Properties of Poly(1-(2-methacryloyloxy)ethyl-3-butyl Imidazolium Bis(trifluoromethanesulfonyl)-imide) Brush Surfaces in an Ionic Liquid. *ACS Appl. Mater. Interfaces* **2010**, *2* (4), 1120−1128.
(25) Asencio, R. A.; Cranston, E. D.; Atkin, R.; Rutland, M. W. Ionic Liquid Nanotribology: Stiction Suppression and Surface Induced Shear Thinning. *Langmuir* **2012**, *28* (26), 9967−9976.
(26) Werzer, O.; Cranston, E. D.; Warr, G. G.; Atkin, R.; Rutland, M. W. Ionic liquid nanotribology: mica−silica interactions in ethylammonium nitrate. *Phys. Chem. Chem. Phys.* **2012**, *14*, 5147−5152.
(27) Bhushan, B.; Palacio, M.; Kinzig, B. AFM-based nanotribological and electrical characterization of ultrathin wear-resistant ionic liquid films. *J. Colloid Interface Sci.* **2008**, *317* (1), 275−87.
(28) Bielecki, R. M.; Crobu, M.; Spencer, N. D. Polymer-Brush Lubrication in Oil: Sliding Beyond the Stribeck Curve. *Tribol. Lett.* **2013**, *49* (1), 263−272.
(29) Bielecki, R. M.; Benetti, E. M.; Kumar, D.; Spencer, N. D. Lubrication with Oil-Compatible Polymer Brushes. *Tribol. Lett.* **2012**, *45* (3), 477−487.
(30) Nalam, P. C.; Daikhin, L.; Espinosa-Marzal, R. M.; Clasohm, J.; Urbakh, M.; Spencer, N. D. Two-Fluid Model for the Interpretation of Quartz Crystal Microbalance Response: Tuning Properties of Polymer Brushes with Solvent Mixtures. *J. Phys. Chem. C* **2013**, *117* (9), 4533−4543.
(31) Hodgman, C. D. *Handbook of Chemistry and Physics*, 20th ed.; Chemical Rubber Publishing Co.: Cleveland, OH, 1948.
(32) Hayduk, W.; Malik, V. K. Density, Viscosity, and Carbon Dioxide Solubility and Diffusivity in Aqueous Ethylene Glycol Solutions. *J. Chem. Eng. Data* **1971**, *16* (2), 143−146.
(33) Pasche, S.; De Paul, S. M.; Voros, J.; Spencer, N. D.; Textor, M. Poly(L-lysine)-*graft*-poly(ethylene glycol) assembled monolayers on niobium oxide surfaces: A quantitative study of the influence of polymer interfacial architecture on resistance to protein adsorption by ToF-SIMS and in situ OWLS. *Langmuir* **2003**, *19* (22), 9216−9225.
(34) Hoh, J. H.; Engel, A. Friction Effects on Force Measurements with an Atomic-Force Microscope. *Langmuir* **1993**, *9* (11), 3310−3312.
(35) Hutter, J. L.; Bechhoefer, J. Calibration of Atomic-Force Microscope Tips. *Rev. Sci. Instrum.* **1993**, *64* (7), 1868−1873.
(36) Green, C. P.; Lioe, H.; Cleveland, J. P.; Proksch, R.; Mulvaney, P.; Sader, J. E. Normal and torsional spring constants of atomic force microscope cantilevers. *Rev. Sci. Instrum.* **2004**, *75* (6), 1988−1996.
(37) Cannara, R. J.; Eglin, M.; Carpick, R. W. Lateral force calibration in atomic force microscopy: A new lateral force calibration method and general guidelines for optimization. *Rev. Sci. Instrum.* **2006**, *77*, 053701.
(38) Hertz, H. On the contact of firm elastic bodies (in German: Ueber die Berührung fester elastischer Körper). *J. Reine Angew. Math.* **1882**, *92*, 156−171.
(39) Li, A.; Benetti, E. M.; Tranchida, D.; Clasohm, J. N.; Schonherr, H.; Spencer, N. D. Surface-Grafted, Covalently Cross-Linked Hydrogel Brushes with Tunable Interfacial and Bulk Properties. *Macromolecules* **2011**, *44* (13), 5344−5351.
(40) Feiler, A.; Plunkett, M. A.; Rutland, M. W. Atomic force microscopy measurements of adsorbed polyelectrolyte layers. 1. Dynamics of forces and friction. *Langmuir* **2003**, *19* (10), 4173−4179.
(41) Donose, B. C.; Vakarelski, I. U.; Higashitani, K. Silica surfaces lubrication by hydrated cations adsorption from electrolyte solutions. *Langmuir* **2005**, *21* (5), 1834−1839.
(42) Bongaerts, J. H. H.; Fourtouni, K.; Stokes, J. R. Soft-tribology: Lubrication in a compliant PDMS-PDMS contact. *Tribol. Int.* **2007**, *40* (10−12), 1531−1542.
(43) Pashley, R. M. Hydration Forces between Mica Surfaces in Aqueous-Electrolyte Solutions. *J. Colloid Interface Sci.* **1981**, *80* (1), 153−162.
(44) Pashley, R. M. Dlvo and Hydration Forces between Mica Surfaces in Li+,Na+,K+,and Cs+ Electrolyte-Solutions - a Correlation of Double-Layer and Hydration Forces with Surface Cation-Exchange Properties. *J. Colloid Interface Sci.* **1981**, *83* (2), 531−546.
(45) Klein, J.; Raviv, U.; Perkin, S.; Kampf, N.; Chai, L.; Giasson, S. Fluidity of water and of hydrated ions confined between solid surfaces to molecularly thin films. *J. Phys.: Condens. Matter* **2004**, *16* (45), S5437−S5448.
(46) Chapel, J. P. Electrolyte Species-Dependent Hydration Forces between Silica Surfaces. *Langmuir* **1994**, *10* (11), 4237−4243.
(47) Ducker, W. A.; Senden, T. J.; Pashley, R. M. Measurement of Forces in Liquids Using a Force Microscope. *Langmuir* **1992**, *8* (7), 1831−1836.
(48) Vigil, G.; Xu, Z. H.; Steinberg, S.; Israelachvili, J. Interactions of Silica Surfaces. *J. Colloid Interface Sci.* **1994**, *165* (2), 367−385.
(49) Valle-Delgado, J. J.; Molina-Bolivar, J. A.; Galisteo-Gonzalez, F.; Galvez-Ruiz, M. J.; Feiler, A.; Rutland, M. W. Hydration forces between silica surfaces: Experimental data and predictions from different theories. *J. Chem. Phys.* **2005**, *123* (3), 034708.
(50) Marcus, Y. Some thermodynamic and structural aspects of mixtures of glycerol with water. *Phys. Chem. Chem. Phys.* **2000**, *2* (21), 4891−4896.
(51) Matsumoto, Y.; Touhara, H.; Nakanishi, K.; Watanabe, N. Molar Excess Enthalpies for Water + Ethanediol, + 1,2-Propanediol, and + 1,3-Propanediol at 298.15-K. *J. Chem. Thermodyn.* **1977**, *9* (8), 801−805.
(52) He, L.; Hu, Y. X.; Wang, M. S.; Yin, Y. D. Determination of Solvation Layer Thickness by a Magnetophotonic Approach. *Acs Nano* **2012**, *6* (5), 4196−4202.
(53) Rosenberg, K. J.; Goren, T.; Crockett, R.; Spencer, N. D. Load-Induced Transitions in the Lubricity of Adsorbed Poly(L-lysine)-*g*-dextran as a Function of Polysaccharide Chain Density. *ACS Appl. Mater. Interfaces* **2011**, *3* (8), 3020−3025.

(54) Grest, G. S. Computer simulations of shear and friction between polymer brushes. *Curr. Opin. Colloid Interface Sci.* **1997**, *2* (3), 271−277.
(55) Lai, P. Y.; Binder, K. Grafted Polymer Layers under Shear - a Monte-Carlo Simulation. *J. Chem. Phys.* **1993**, *98* (3), 2366−2375.
(56) Irfachsyad, D.; Tildesley, D.; Malfreyt, P. Dissipative particle dynamics simulation of grafted polymer brushes under shear. *Phys. Chem. Chem. Phys.* **2002**, *4* (13), 3008−3015.
(57) Kreer, T.; Binder, K.; Muser, M. H. Friction between polymer brushes in good solvent conditions: Steady-state sliding versus transient behavior. *Langmuir* **2003**, *19* (18), 7551−7559.
(58) Klein, J.; Perahia, D.; Warburg, S. Forces between Polymer-Bearing Surfaces Undergoing Shear. *Nature* **1991**, *352* (6331), 143−145.